CrystEngComm

Accepted Manuscript

This article can be cited before page numbers have been issued, to do this please use: X. Fan, J. Geng, N. Soin, S. Chakrabarti, S. Mitra, I. Roqan, H. Li, M. O. Babatunnde and A. Baldwin, *CrystEngComm*, 2021, DOI: 10.1039/D1CE00413A.

ROYAL SOCIETY OF CHEMISTRY

rsc.li/crystengcomm

View Article Online
DOI: 10.1039/D1CE00413A

ARTICLE

A Solid-liquid Two-phase Precipitation Method for Growth of Fullerene (C_{60}) Nanowires

Received 00th January 20xx,
Accepted 00th January 20xx

DOI: 10.1039/x0xx00000x

Xiao Fan,[a] Junfeng Geng,*[a] Navneet Soin,*[b] Supriya Chakrabarti,[b] Somak Mitra,[c] Iman S. Roqan,[c] Hua Li,[d] Mustapha Olaoluwa Babatunde,[a] and Andy Baldwin[a]

A novel solid-liquid two-phase precipitation (SLTPP) method, utilising a solidified (*via* liquid N_2) m-xylene solution of C_{60} with liquid isopropanol (IPA) as the counter-solvent, is proposed for the synthesis of fullerene (C_{60}) nanowires. The resulting C_{60} nanowires were observed to possess high crystallinity, a length-to-diameter ratio of up to several thousand with a diameter as small as ~ 85 nm. We further systematically investigated the effects of C_{60} concentration (1 – 5.2 mg/ml) and solvent – counter-solvent ratio (1:6 – 2:1) to optimise the growth conditions for high-quality, size-controlled C_{60} nanowires. A comparative study against the widely-used liquid-liquid interfacial precipitation (LLIP) method showed that the proposed SLTPP method led to a much narrower diameter distribution (414.20 ± 92.10 nm *vs.* 3237.20 ± 1790.30 nm for LLIP) across the studied range of C_{60} concentration and solvent – counter-solvent ratio, and is therefore considered to be a more stable and reliable synthesis route. We propose that the gradual melting of the m-xylene C_{60} solid-phase leads to a slower diffusion of the solvent – counter-solvent medium, providing a much more stable interface for high-quality crystal growth.

Introduction

Fullerene (C_{60}) nanowires, as one-dimensional nanostructures of C_{60}, have attracted great attention due to their outstanding physio-chemical properties and potential applications.[1] Besides possessing the molecular properties of the parent C_{60} molecule – such as the nonlinear properties in the excited triplet state and photo-transformation,[2] the C_{60} nanowires exhibit unique properties associated with their high surface area, low-dimensionality, and potential quantum confinement effect, which make them potentially suitable for applications such as optical limiters,[2,5] photoconductors for solar energy devices,[6, 7] field-emission transistors,[8,9] nanoprobes,[10] high-frequency filters,[10] and targeted drug-delivery vehicles.[11-13] As the C_{60} nanowires are largely composed of carbon with only a very tiny amount of hydrogen in their crystal structure,[3] they are expected to exhibit excellent bio-compatibility[14-16].

The vapor-driven crystallization and solution-driven self-assemblies such as interfacial precipitation, template-assisted dip drying[17] and drop drying process[18] are some of the important methods which have developed for the assembly of C_{60}.[19] For C_{60} nanowires, the morphology, crystallinity, and indeed their size, diameter is dependent on the synthesis route and as such significant efforts have been devoted to study the fundamental synthesis routes and their corresponding growth mechanisms.[20,21] As a result, over the years, the following two synthesis methods have gained prominence for the synthesis of C_{60} nanowires: (i) direct solution growth method and (ii) liquid-liquid interfacial precipitation (LLIP).

The direct solution growth/evaporation method for C_{60} nanowire growth[3,22-24] proceeds *via* slow evaporation of the organic solvent phase of the C_{60}-organic solvent solution (typically CH_2Cl_2,[25] m-xylene,[18] 1,2,4-trimethylbenzene[3] and m-dichlorobenzene[24]). For such processes, the aspect ratio (length/diameter) is typically controlled by varying the evaporation rate and choice of solvent.[24] In fact, some of the early experiments on C_{60} crystal growth utilised slow evaporation of C_{60} solutions to grow crystals of micro- to milli-meter sizes.[24] The incorporation of solvent molecules into the C_{60} nanowire crystal lattice is an unavoidable consequence of the process and leads to formation of various crystalline forms including needle-like and nanosized wire-like C_{60} crystals. As the process relies on an interplay of C_{60} concentration, its solubility in organic solvent, and the evaporation temperature of solvent, it was observed that a certain critical concentration is required for the C_{60} molecules to initiate small clusters / aggregation which eventually leads to the formation of C_{60} nanowires.[24] At the same time, the very nature of the process is time-

[a] *Institute for Materials Research and Innovation (IMRI), School of Engineering, University of Bolton, Bolton BL3 5AB, United Kingdom. E-mail: j.geng@bolton.ac.uk*
[b] *School of Engineering, Ulster University, Newtownabbey, Belfast BT37 0QB,* Northern Ireland, United Kingdom. *E-mail: n.soin@ulster.ac.uk*
[c] Division of Physical Sciences and Engineering, King Abdullah University of Science and Technology (KAUST), Thuwal, 23955-6900 Kingdom of Saudi Arabia
[d] College of Life and Environmental Sciences, Minzu University of China, Beijing, China
Electronic Supplementary Information (ESI) available: [details of any supplementary information available should be included here]. See DOI: 10.1039/x0xx00000x

consuming, generally taking several weeks to obtain abundant nanowires.[3,26]

On the other hand, in the LLIP method proposed by Miyazawa et al., uses a solvent, counter-solvent interaction to form an interface where low-dimensional C_{60} nanostructures such as nanowires and tubular crystals can grow.[2730] In their work, C_{60} nanowires were obtained at the isopropanol (IPA)/toluene interface where the slow addition of IPA to the toluene C_{60} solution resulted in the formation of fine needle-like crystals of submicron diameter C_{60} which could reach a maximum length 10 mm after 53 h of growth.[27] In the LLIP process, several factors can be varied including concentration, solvents,[31,32] total solvent volume,[33] solvent volume ratio,[34] illumination conditions[35] and more recently, fullerene derivatives themselves.[36] For example, the addition of IPA or tetra-butyl alcohol to the saturated C_{60} solutions prepared in benzene, toluene or in carbon tetrachloride resulted in the formation of 2D crystals instead of nanowires.[32] Owing to the low solubility of C_{60} in alcohols, they are primarily used as counter-solvents and thus the crystal-formation mechanism is supersaturation driven, requiring that the differences between the solubility of C_{60} in the counter-solvent and a good/better solvent be taken into account.[20] The modification of such liquid/liquid interface can trigger the formation of C_{60} self-assembly and thus provides a pathway to tailor various nanostructures including C_{60}–C_{70} two-component fullerene nanowires and K-doped C_{60} nanowires.[1] However, for self-assembly processes like LLIP, due to the complex interplay of aforementioned decisive factors, it is very difficult to obtain nano- and microstructures with pre-determined morphologies[19] and uniformity.

Invariably, both the LLIP and direct solution growth methods suffer from their own unique drawbacks. For instance, the large-scale production of C_{60} nanowires *via* the direct solution evaporation process is particularly time-consuming as compared to the 'quick' LLIP method and requires 1-3 days or more. However, for LLIP method it is difficult to control the size and uniformity of the C_{60} nanowires owing to the difficulties encountered in obtaining a sharp and clear interface of the two solvents during liquid-liquid diffusion.[37] In LLIP, giant rod-like C_{60} crystals, and crystals of other shapes, are frequently observed mixed with the nanowires, necessitating effective separation methods and adding further complexity to the process. Besides, the LLIP method is not very versatile as the variation of counter-solvent (methanol, ethanol, isopropanol, etc.) has been shown to not affect the diameter distribution significantly.[24]

In this work, through a solid-liquid two-phase precipitation (SLTPP) process, we report a new method of synthesising C_{60} nanowires with good morphological uniformity, diameter as small as ~ 85 nm, and length-to-diameter ratio as large as several thousand. By varying the C_{60} concentration (1 – 5.2 mg/ml) and solvent – counter-solvent ratio (1:6 – 2:1), we have investigated thoroughly the optimal growth conditions for high-quality, size-controlled C_{60} nanowires. We have characterized the synthesised nanowires through Raman analysis, infra-red spectroscopy, electron microscopy, and thermal analysis to determine the composition of the C_{60} nanowires. A further

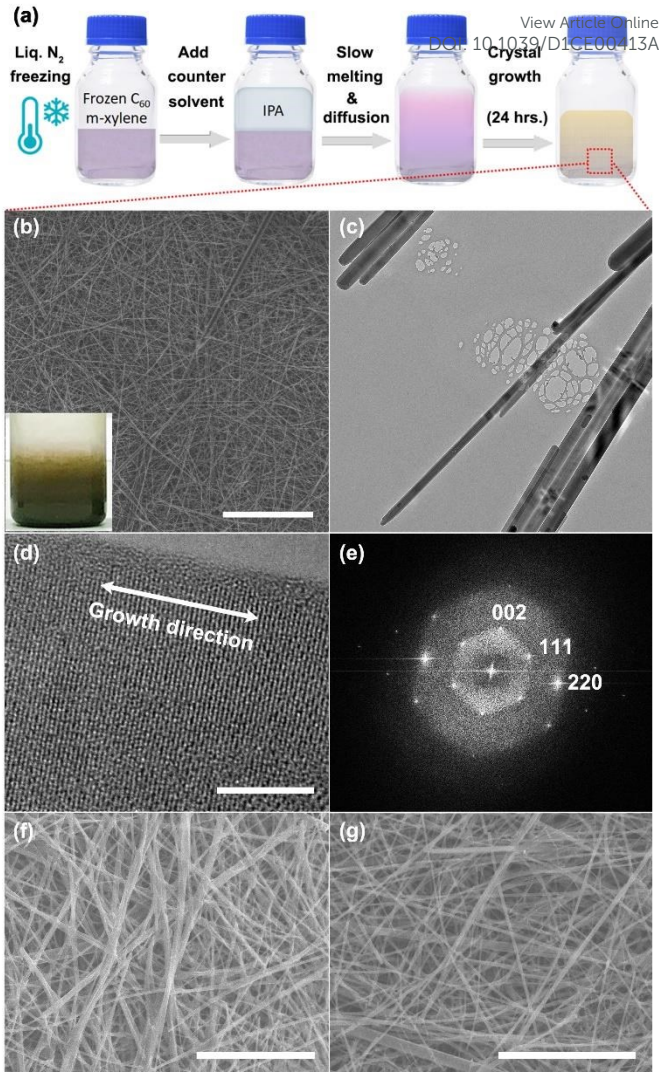

Fig.1 (a) Schematic diagram of steps undertaken during the SLTPP process, (b) SEM image of C_{60} nanowires prepared by the SLTPP method using m-xylene/IPA solvent system with a total volume of 6 mL, scale bar: 50 µm; (c) TEM image of fine C_{60} nanowires, scale bar: 1 µm; (d) HRTEM image of an as-prepared nanowire, scale bar: 10 nm; (e) FFT image for (c); typical high magnification SEM images of C_{60} nanowires prepared on (f) small scale with a total volume of 6 mL and (g) large scale with a total volume of 40 mL, respectively, scale bars: 20 µm. The inset is a digital photograph of the growth of C_{60} nanowires imaged in (b), in this case the nanowires were deposited at the bottom of the vial after 24 h of growth.

comparison against the widely used LLIP method was carried out at various C_{60} concentrations (1 – 5.2 mg/ml) and solvent – counter-solvent ratios (1:6 – 2:1) to ascertain the applicability of the method. For the growth conditions studied, it was observed that not only the SLTPP method provided a much tighter control over the diameter than the LLIP method, and the diameter variability was significantly smaller.

Experimental

Materials & Method

C_{60} nanowires were prepared using m-xylene and IPA as solvent and counter-solvent, respectively. A typical procedure is as

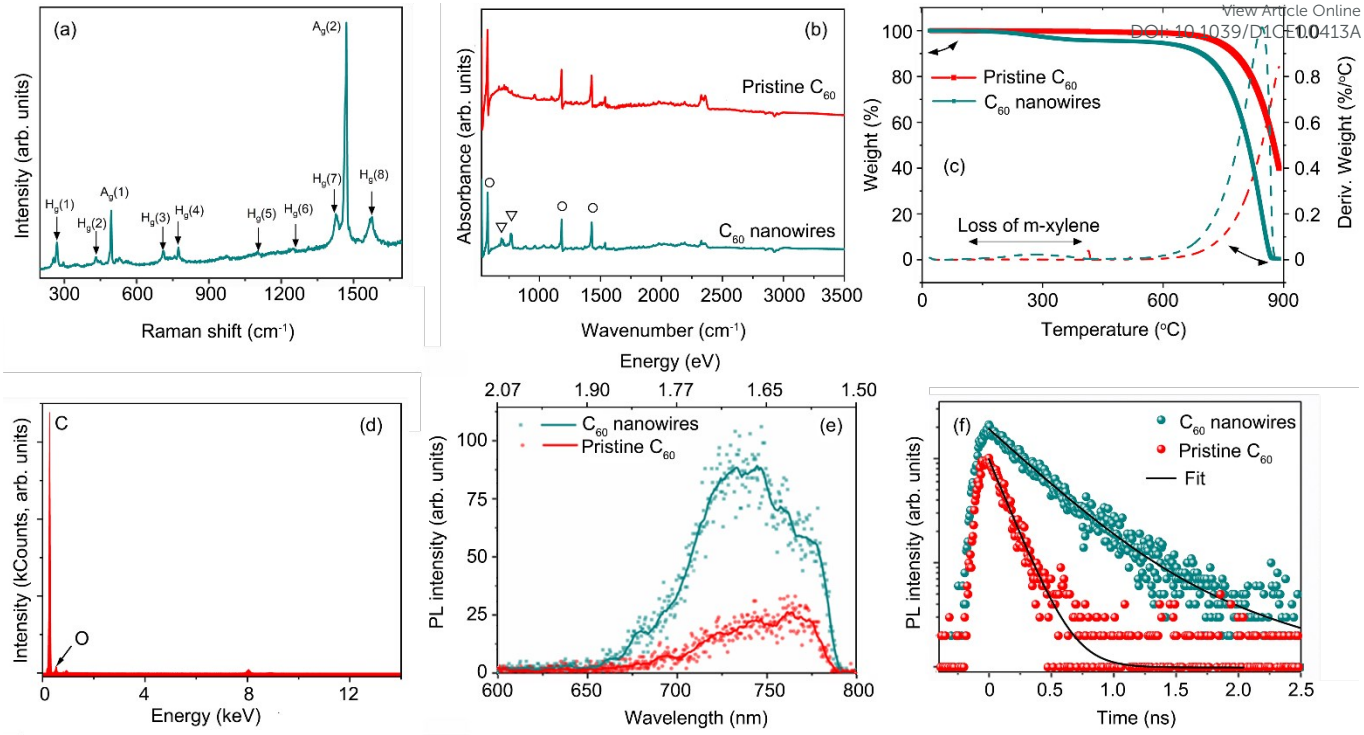

Fig. 2 (a) A typical Raman spectrum of C_{60} nanowires made by the SLTPP method using the m-xylene/IPA solvent system; (b) FTIR spectra of the pristine C_{60} powder and the as-prepared C_{60} nanowires; (c) TGA and DTG curve of the as-prepared C_{60} nanowires, together with those obtained from raw 99.5% C_{60} powder (for comparison); (d) EDS spectrum of the as-prepared C_{60} nanowires; (e) PL spectra of pristine C_{60} and C_{60} nanowires prepared using SLTPP method and (f) Time-resolved photoluminescence (TRPL) spectra of pristine C_{60} and C_{60} nanowires and their fitting curves (solid black lines), λ_{ex} = 400 nm (note the y-axis is a logarithmic scale).

follows. 1.5 mL of C_{60} solution in m-xylene (concentration: 2 mg/mL) was prepared by dissolving the as-received C_{60} powder (99.5%, Alfa Aesar) in pure m-xylene (99+ %, ACROS Organics) and poured into a 10 mL volume transparent glass bottle. The glass bottle was then slowly and carefully immersed into a liquid nitrogen (N_2) dewar, up till the level of C_{60} solution. Once the purple coloured C_{60} solution was completely frozen by liquid N_2, 4.5 mL of IPA (99.6%, ACROS Organics) (1:3 volume ratio) was added to the bottle. The bottle was then immediately capped and stored at in a freezer (maintained at -8 °C) for ~24 h for the synthesis of C_{60} nanowires. The obtained nanowires filtered and washed with ethanol, and then dried overnight at room temperature. A relatively large-scale synthesis of C_{60} nanowires was also carried out using 10 mL C_{60}- m-xylene solution (2 mg/ml) and 30 mL IPA *via* the same procedure as described above to ascertain the scalability of the process.

Characterisation

The morphology of as-prepared C_{60} nanowires was characterized by scanning electron microscopy (SEM, Hitachi S-3400N) at an accelerating voltage of 10 kV and transmission electron microscopy (TEM) on a JEOL-2100F at an accelerating voltage of 200 kV. For SEM, the samples were deposited onto a conductive carbon tape attached on the specimen holder. For TEM, the C_{60} nanowires were dispersed in IPA with gentle shaking to avoid any damage to the nanocrystals, and a drop of such suspension was placed onto a holey carbon film on a 300-mesh copper grid (Agar) and dried in air at room temperature. Raman spectra were recorded on a Horiba Xplora spectrometer with an excitation laser of 532 nm wavelength and a spot size less than 1 µm. The laser power was controlled at a low level of 8 µW to prevent photo-polymerisation. Fourier Transform Infrared Spectroscopy (FTIR) was performed on both pristine C_{60} powders and C_{60} nanowires using a Thermo Scientific Nicolet iS10 spectrometer with OMNIC software. Air-dried C_{60} nanowire samples were deposited directly on top of the sample holder for carrying out the analysis. Thermal gravimetrical analysis (TGA) was performed using SDT Q600 V20.9 instrument with a microbalance of 1 µg resolution and equipped with Universal Analysis software. The TGA was carried out in N_2 atmosphere at a flow rate of ~100 mL/min between room temperature and 900 °C at a ramp rate of 20 °C/min. The photoluminescence (PL) and ultrafast dynamics of photocarriers of the samples was studied using wavelength-integrated time-resolved photoluminescence (TRPL) down to the sub-nanosecond regime. PL and TRPL measurements were performed with a mode locked Ti:sapphire laser (Coherent Mira 900). Laser excitation power on the sample was kept constant at 1.5 mW and laser beam size was 60 µm in diameter on the sample. A second harmonic generator (APE-SHG /THG) was used to excite the sample by output wavelength of 400 nm (pulse width 150 fs, pulse repetition rate of 76 MHz). Sample emission was detected by a monochromator attached to a Hamamatsu C6860 streak camera with a temporal resolution of 2 ps.[38,39]

Results and discussion

Morphology and microstructure

At the end of the synthesis process, significant amounts of golden-brown-coloured suspension (a signature of the C_{60} nanowires) were observed in the lower part of the glass bottles (inset of Fig. 1(b)). SEM images (Figs. 1(b, f)) indicate that the suspension typically comprised of wire-like C_{60} nanocrystals with a typical diameter of 150-600 nm and a length of hundreds of micrometres, and thus a length-to-diameter aspect ratio of up to several thousand. The diameters of 125 such C_{60} nanowires from the sample were measured by SEM and the mean diameter was calculated to be 327.4 ± 164.6 nm. TEM image presented in Fig. 1(c) shows fine C_{60} nanowires with diameter ranging from 85-275 nm. High-resolution TEM image (HRTEM) shows lattice fringes of a such nanowire with the corresponding Fast Fourier Transform (FFT) image (Fig. 1(e)) confirming the crystalline structure of a nanowire where the measured *d*-spacings of d(002) = 7.6 Å, d(220) = 5.0 Å and d(111) = 8.3 Å, indicate a face-centred cubic (fcc) structure for the obtained C_{60} nanowires.[40-42]

To assess the viability and scalability of the process, synthesis was also carried out using a larger solution volume (10 ml C_{60} / 30 ml IPA) in appropriate-sized glass containers. No obvious morphological differences were observed, except for a slightly smaller mean diameter of ~ 296 nm for the large-batch sample (Fig. 1(g)) as compared to ~327 nm for the small-batch sample (Fig. 1(f)). This difference could arise from minor solvent effect and interface formation but overall, the growth results obtained at different production scales were consistent with each other. It was noted that along with the long and thin C_{60} nanowires, a small amount of rod-like C_{60} crystals were found for both large-scale and small-scale samples. These rod-like crystals were normally 1-2 µm in diameter, with a few up to about 3.5 µm in diameter, and less than 150 µm in length.

Micro-Raman spectroscopy was performed on the as-prepared C_{60} nanowires. As shown in Fig. 2(a), there were eight Raman bands corresponding to active H_g modes of C_{60} at 269, 431, 709, 774, 1100, 1249, 1428, and 1572 cm^{-1}. The two strongest Raman bands were corresponding to the two A_g modes of C_{60} at 493 and 1469 cm^{-1}. The observed A_g and H_g bands prove conclusively that the nanowires were composed of C_{60} molecules. It is understood that the presence of trace quantity of solvent molecules can enhance the photo-assisted polymerization of the C_{60} molecules which leads to the blue-shift of the Raman band to ~1459 cm^{-1} from its original position of 1469 cm^{-1}.[7, 43] The absence of this shifted $A_{g(2)}$ band indicates that the hierarchically-organised nanowires contain non-polymerised, monomeric C_{60} molecules which are held together by van der Waals forces.[35]

Owing to the low exciton population for radiative recombination, the optical properties of pristine fullerenes have not attracted significant interest.[44,45] As such the PL of C_{60} molecules is weak, due to optically forbidden transition between the lowest unoccupied molecular orbital (LUMO) and the highest occupied molecular orbital (HOMO).[46,47] However, recent studies have shown enhanced PL and fluorescence from self-assembled molecular structures such as C_{60} aggregates,[48]

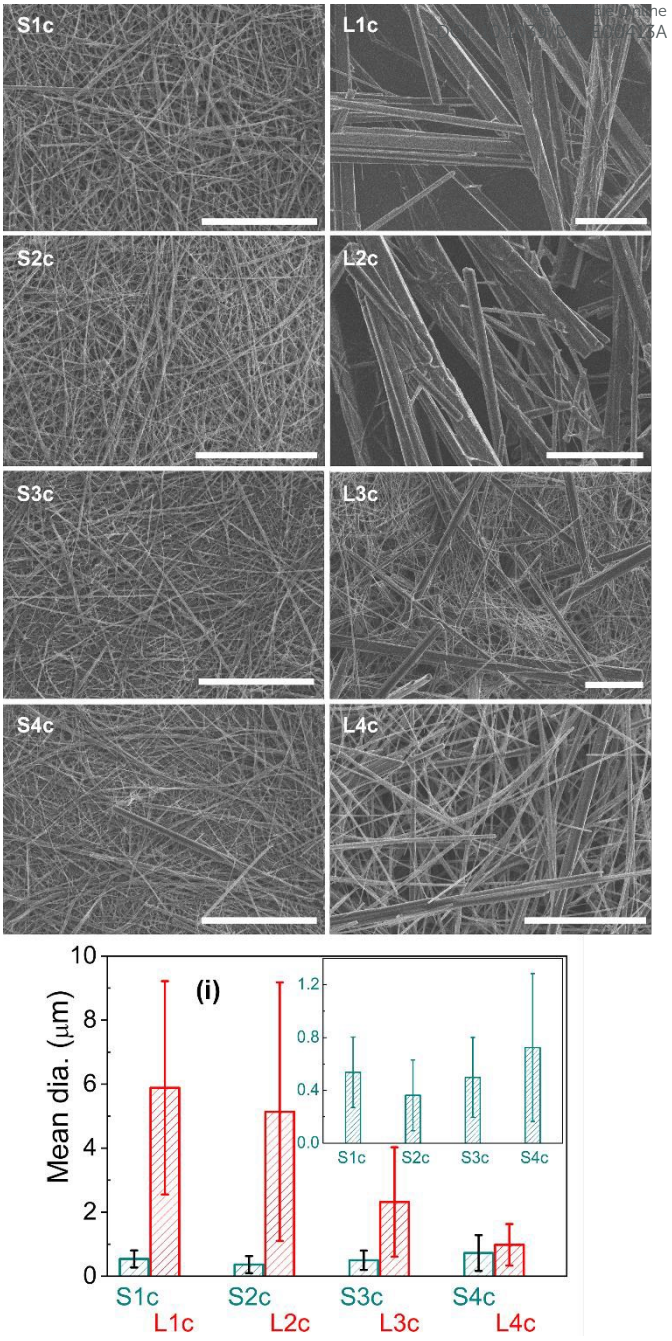

Fig. 3 SEM images of C_{60} nanowires prepared using m-xylene/IPA system through the SLTPP method and the LLIP method with C_{60} concentrations of 1 mg/mL, 2 mg/mL, 3 mg/mL and ~5.2 mg/mL, respectively. Scale bars: 50 µm. (i) Histograms of mean diameters of 125 C_{60} wire-like crystals prepared by the SLTPP and LLIP method with C_{60} concentrations of 1, 2, 3 and ~5.2 mg/mL, respectively. Inset shows the diameter distribution of samples from SLTPP method.

C_{60} nanowires[18,49] and C_{70} nanocubes, which usually have an intrinsically low emission while existing in solutions or powders. In our work, both the pristine C_{60} and C_{60} nanowires show a weak, broad PL spectrum (Fig. 2(e)) which arises due to the size distribution of the C_{60} crystals (i.e., the diameter or the wall thickness of nanowires).[49] The typical PL energies for our samples ranged from 1.62 eV (for pristine C_{60}) to ~1.66 eV (for C_{60} nanowires), which matches well with the earlier reported

View Article Online
DOI: 10.1039/D1CE00413A

values.[48,49] This observed blue-shift of the C_{60} nanowires and simultaneous PL enhancement as compared to the pristine C_{60} has been reported earlier by Shreshta et al.[49] in their work on surfactant-assisted LLIP method, and for the C_{60} nanowhiskers, nanotubes[50] and other 1D organic crystals.[51] In their work, Wang et al.[18] have suggested that the van der Waals type of interaction between C_{60} and solvent molecules reduces the icosahedral symmetry of C_{60} molecules and induces strong PL from solvated C_{60} nanorods. Similarly, it is known that the HOMO-LUMO transitions in molecular semiconductors are highly sensitive to the proximity of proximal molecules, therefore the observed blue shift in the PL spectra of the SLTPP synthesised C_{60} nanowires can be attributed to the solvated crystals (arising from the incorporation of m-xylene molecules, discussed in the next section) and the defects in such crystal structures including dislocations and stacking faults.[18] The excited state dynamics of the pristine C_{60} and C_{60} nanowires was further investigated using TRPL measurements, where the decay of the PL intensity with time indicates the quenching of photogenerated carriers owing to recombination. As shown in Fig. 2(f), the decay of PL in pristine C_{60} can be represented by a single-exponential function with a lifetime of $\tau = 0.15$ ns around 740 nm (excitation wavelength $\lambda_{ex} = 400$ nm), while the C_{60} nanowires display a bi-exponential PL decay with lifetimes of $\tau_{fast} = 0.39$ ns and $\tau_{slow} = 1.7$ ns. While the observed PL originates from the transition of the first excited singlet state S1 to the ground state S0, the slow decay process observed for the C60 nanowires is understood to arise from a weakly allowed intramolecular transition and/or interactions between the C_{60} and m-xylene molecules present in the nanowire structure.[52] Similar lifetime values were observed by Byrne et al.[53] and Jie et al.[54] for C_{60} single crystals and films, respectively.

Chemical Composition

According to previous studies, C_{60} nanowires prepared by both the evaporation method and the LLIP method contain a small amount of solvent molecules.[3,24,31,55,56] Therefore, it is reasonable to assume that C_{60} nanowires prepared by our SLTPP method contain either m-xylene or IPA molecules, or both. EDS spectrum, as seen in Fig. 2(b), of a C_{60} nanowire shown in Fig. 1(b) prepared by the SLTPP method using m-xylene/IPA solvent system shows a sharp peak of carbon. This may be considered in conjunction with the Raman spectrum of C_{60} nanowires (Fig. 2(a)), where no obvious peak corresponding to either m-xylene molecules or IPA molecules was observed, possibly because the number of solvent molecules encapsulated in the crystal lattice was very small.

To determine if the guest solvent molecules were present in the nanowire samples, further FTIR measurement were performed on as-prepared C_{60} nanowires, and the resulting FTIR spectra are presented in Fig. 2(c). The appearance of peaks of C_{60} at 525, 575, 1182 and 1428 cm^{-1} (attributed to C-C vibrational modes and marked as circles), arising from the three-fold degenerate first-order dipole active T_{1u} modes,[57] confirmed that these wire-like nanocrystals were indeed composed of C_{60} molecules. We also observed characteristic peaks corresponding to C-H bonding and the ring band in m-xylene at 688 and 766 cm^{-1}, respectively (marked as triangles), which prove the existence of m-xylene molecules in the nanowire structure.[31] The lack of the broad O–H (~3450 cm^{-1}) and C-OH stretching peaks (at ~1107 cm^{-1}) further confirm that the starting C_{60} powders were of high purity. Although some previous studies have reported on the existence of guest counter-solvent molecules in C_{60} rods synthesized by the LLIP method,[18] however, no peaks corresponding to IPA anti-solvent (e.g. C-C-O symmetric stretching vibration at 817 cm^{-1} or broad O-H stretch band at over 3000 cm^{-1}) could be found in FTIR spectrum for our samples. This suggests that only m-xylene molecules were encapsulated in the crystal lattice of C_{60} nanowires made by our SLTPP method. Some signature of this inclusion could also be observed in the Raman spectra where the slight downshift of $H_g(1)$ and $A_g(1)$ modes to 269 and 493 cm^{-1} as compared to those of pristine C_{60} powder at 273 and 497 cm^{-1},[58] respectively, suggesting the possible existence of solvent molecules in the crystal lattice which reduce the symmetry of C_{60} molecules or may arise from the photoreaction between excited C_{60} and neighbouring molecules occurring *via* laser irradiation during measurements.[49]

To determine the ratio of m-xylene to C_{60}, TGA and its corresponding derivative thermogravimetry (DTG) analysis were performed on the as-prepared nanowires in a N_2 atmosphere (Fig. 2(d)). It was expected that two mass-loss stages up to 900 °C should occur which were indeed observed. The first mass loss started at ~150 °C which is close to the boiling temperature of m-xylene, and ended at ~400 °C, with a maximum mass loss rate occurring at ~275 °C. Thus, this stage of mass loss can be clearly attributed to the removal of the guest m-xylene molecules from the C_{60} nanowires. However, no indication of the existence of IPA molecules could be ascertained due to lack of mass-loss peak around 82.5 °C (boiling point of IPA). This result is consistent with that of the micro-Raman and FTIR analysis. The second stage of mass loss occurred at much higher temperatures starting from ~620 °C, ascribed to the sublimation of C_{60} molecules, which agrees well with the TGA result of pristine C_{60} powders. Moreover, the TGA result indicated that the weight loss percentage of m-xylene solvent and C_{60} molecules was ~5% and ~95%, respectively. Based on this result, the molar ratio of m-xylene to C_{60} in the sample was estimated to be ~1:3.

Effect of concentration of C_{60} on the growth of C_{60} nanowires

For the LLIP method, it has been reported that C_{60}-saturated solutions are essential for the synthesis of fullerene nanowires.[7,28,32,59,60] However, using the SLTPP method, it was observed that C_{60} nanowires with good diameter uniformity can be successfully grown using an unsaturated C_{60} solution even at low starting concentrations. To investigate the dependence of the nanowire growth behaviour on the starting solution concentration, a comparative study was carried out using both SLTPP and LLIP methods. For this, a series of C_{60} solutions in m-xylene at concentrations of 1, 2 and 3 mg/mL and a C_{60} -saturated m-xylene solution (~5.2 mg/mL), with a fixed volume

ratio of C_{60} to IPA of 1:2 was prepared (Table S1 in Supplementary Information). For the SLTPP process (samples named as S#c), following the freezing action on the solution by liquid N_2 and the subsequent addition of IPA into the growth vials, an abundance of yellow-brown substances initially appeared at the solid-liquid interface. After ~2 h, a complete precipitation of yellow-coloured substances corresponding to C_{60} nanowires from C_{60}-saturated m-xylene solution was observed (sample S4c), while the purple-colour of the initial C_{60} solutions could still be observed for samples S1c, S2c and S3c where the starting C_{60} concentration was low (1, 2 and 3 mg/mL, respectively). However, after ~24 h, abundant yellow-coloured C_{60} nanowires were observed for these low-starting concentration samples S1c, S2c and S3c, and no obvious purple colour of the starting solutions could be observed at this point (see Fig. 1, Fig. S2 and Table S1).

In contrast, under identical conditions, the growth *via* the LLIP method (samples named as L#c) was slower than that of the SLTPP method (Fig. S3 and Table S1). While yellow-brown coloured C_{60} nanocrystals precipitated completely after 24 h in high concentration samples L3c and L4c, the purple colour corresponding to starting solutions could still be clearly seen in the lower part of the vials of low starting concentration samples L1c and L2c, indicating an incomplete precipitation (Fig. S3 and Table S1) and thus a slower growth rate than samples S1c and S2c. It was also observed that for the low-concentration LLIP samples (L1c), a very small amount of C_{60} nanocrystals could be observed, thus pointing at the significant differences in the growth mechanisms and growth rates of the LLIP method vis-à-vis the SLTPP method. Moreover, it was observed that after complete precipitation from all these samples, C_{60} nanocrystals prepared by the SLTPP method possessed a yellow colour, while those from the LLIP method were a mixture of yellow-brown substances and large, black-coloured, needle-like crystals.

To ascertain the differences between the two methods, diameters of over 125 C_{60} nanocrystals from each sample were measured by SEM and their mean diameter calculated. As shown in SEM images of Fig. 3 and histogram (inset) of Fig. 3(i), no significant difference in size was observed in samples S1c, S2c and S3c, but a small number of rod-like crystals with a diameter as large as 3.5 µm was found in S4c. With the increase of C_{60} concentration, the C_{60} nanowires prepared by the SLTPP method showed no obvious change in size and shape, showing a consistent uniformity in size and shape regardless of the solution concentration, and hence provides a tighter control on the quality of C_{60} nanowires. In comparison, the LLIP method is more sensitive to the solution concentration, with the diameter showing an inverse dependence on the solution concentration (Fig. 3(i)). Thus, it can be argued that the SLTPP method is much more robust and stable than the LLIP method in its ability to nucleate and grow the C_{60} nanowires even at low starting C_{60} concentrations.

We propose the following mechanism to explain the significant differences observed for the effect of concentration on the C_{60} nanowires grown via STLPP and LLIP methods. The crystal growth in the LLIP method is driven by pressure across the liquid-liquid interface due to different viscosities and surface

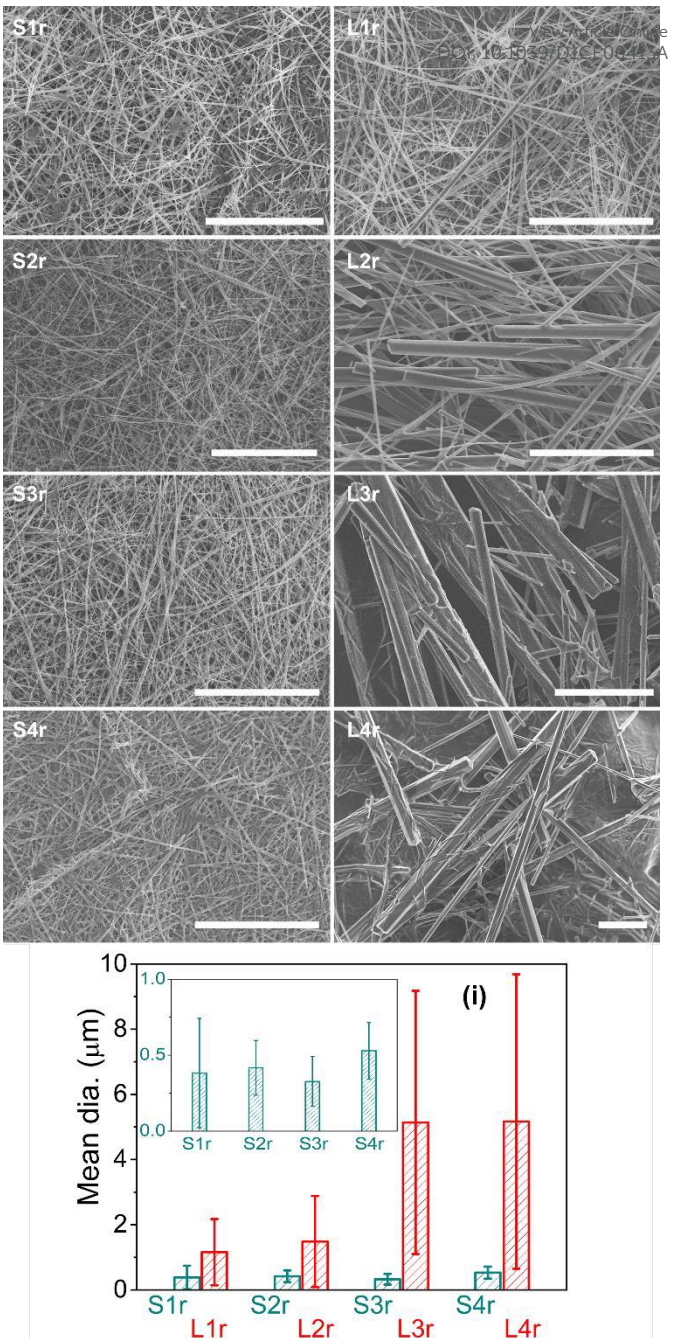

Fig. 4 SEM images of C_{60} nanowires prepared using m-xylene/IPA system through the SLTPP method and the LLIP method with m-xylene to IPA volume ratio of 1:6, 1:4, 1:2 and 1:1, respectively. Scale bars: 50 µm. (i) Histograms of mean diameters of 125 C_{60} wire-like crystals prepared by the SLTPP and LLIP method with varying m-xylene to IPA volume ratio. Inset shows the diameter distribution of samples from SLTPP method.

tensions between the two liquids,[61] where a reduction of C_{60} concentration leads to a decrease in liquid-liquid interfacial pressure. However, in the SLTPP method, the C60 concentration has little effect on the interfacial pressure because the starting C_{60} solution is already frozen into a solid phase prior to the addition of the second solvent into the growth system. In SLTPP method, although a liquid-liquid interface gradually forms following the melting of the solid phase, the diffusion rate of the

two liquids would be much slower than that of the LLIP process. It has been shown previously by Ringor and Miyazawa[62] that lower temperatures reduce the solubility of C_{60} molecules in the solvent-counter solvent mixture, producing a larger number of fullerene nanotubes, albeit with a wider variation in diameter distribution. We therefore expect that for the SLTPP method, the frozen C_{60} solution provides an even slower diffusion, allowing for the nucleation of a large number of nanotubes. Moreover, the interface formed in the SLTPP method is much more stable than that of the LLIP method because of the fact that half of the growth system was in solid state at the early stage of the growth. The combination of the slower diffusion rate and a more stable interface makes the nanowire growth process more controllable and less dependent on the concentration of the solution in the SLTPP process. Consequently, the SLTPP method appears to be a better choice over the LLIP method for the synthesis of high quality C_{60} nanowires with a significantly tighter control over the diameter.

Effect of solvent volume ratio on C_{60} nanowires

A series of samples, as shown in Table S2, with a fixed C_{60} concentration of 2 mg/mL and various volume ratios (1:6 to 2:1) of solvent (m-xylene) to counter-solvent (IPA) were prepared to investigate the effect of solvent to counter-solvent ratio on the C_{60} nanowire growth *via* both the SLTPP (sample name as S#r) and LLIP (sample named as L#r) methods. It was observed that within a 2-hour growth period, using the SLTPP method, the C_{60} solution for sample S1r with a ratio of 1:6 turned into a yellow-brown substance completely, while the dark purple-coloured C_{60} solution remained for samples with ratios of 1:4, 1:2, 1:1 and 2:1 (S2r, S3r, S4r, and S5r, respectively). Similarly, the dark purple colour of the starting solution remained for all the samples prepared through the LLIP method. Only after 24 h, the precipitation of yellow brown C_{60} nanowires was observed from samples (S1r, S2r, L1r and L2r) with ratios of 1:6 and 1:4 prepared through both the SLTPP method and the LLIP method. A small amount of purple-coloured liquid was observed for samples S4r and S5r, while a large amount of the pristine C_{60} solution was observed in sample L3r, L4r and L5r (see Fig. S4 and Table S2). After one week of growth, yellow crystals were found in all samples prepared through the SLTPP method, while those obtained through the LLIP method showed a brown-black colour, and the purple-colour of the starting C_{60} solution in samples S4r, S5r, L4r and L5r did not disappear completely (see Fig. S5 and Table S2). The result indicates that under identical experiment conditions, a relatively low C_{60} solution-to-IPA volume ratio can initiate fast nucleation and thus subsequent growth of C_{60} nanowire through both the SLTPP and the LLIP methods, however, the growth of C_{60} nanowires though the SLTPP method was quicker than that of the LLIP method. C_{60} crystals prepared through the SLTPP method presented a bright yellow colour corresponding to C_{60} nanowires, while those prepared through the LLIP method were much darker, especially when the samples were made with high volume ratios, indicating that they were crystals with larger size.

The morphologies of C_{60} nanowires grown by both SLTPP method and LLIP method are shown in Fig. 4. To ascertain the differences between the two methods, we again measured the diameters of over 125 C_{60} crystals by SEM and calculated the mean diameter value (Fig. 4(i)). It was observed that for samples grown through SLTPP method, with the change in the volume ratio from 1:6 to 1:2, the shape and size of the C_{60} nanocrystals remained largely unchanged as shown in Fig. 4(i). For samples prepared by the LLIP method, solvent ratio can significantly affect the morphology of C_{60} nanowires. For example, C_{60} nanowires were clearly observed in sample L1r, but giant rod-like crystals with diameter as large as 20 µm were the dominant feature in sample L2r although a very small amount of C_{60} nanowires were found there. Meanwhile, no nanowires but only large crystals were observed in samples L3r and L4r.

Conclusions

C_{60} nanowires with diameter as small as ~85 nm, mean diameter of 327.4 ± 164.6 nm and length-to-diameter ratio up to several thousands have been successfully synthesized in this work through a solid-liquid two-phase precipitation method. The crystal structure and chemical composition of such grown nanowires have been studied by spectroscopic and electron microscopy techniques. By observing the C_{60} nanowires prepared through the SLTPP method under different conditions, we observed that the growth efficiency of C_{60} nanowires improves with the reduction of m-xylene to IPA volume ratio and the increase of C_{60} concentration, while a relatively high-volume ratio of 1:2 and low C_{60} concentration of 2 mg/mL leads to the best uniformity in fine C_{60} nanowires with highest length-to-diameter ratio. Considering both the growth efficiency and morphological control of C_{60} nanowires, we conclude that the optimal growth conditions are 2-3 mg/ml of C_{60}-m-xylene and m-xylene:IPA ratio of 1:2, respectively. Based on a comparative study with currently widely used LLIP method under identical experiment conditions, we further conclude that the SLTPP method is much less sensitive to the solvent to counter-solvent ratio and the starting C_{60} concentration in the solution. Hence, the SLTPP method is a more stable and reliable method for growing uniform-sized and uniform-shaped C_{60} nanowires in a controlled manner. Future work will look at establishing the empirical principles and a complete growth mechanism for the SLTPP method.

Conflicts of interest

There are no conflicts of interest to declare.

References

1 X. Fan, N. Soin, H. Li, H. Li, X. Xia and J. Geng, *Energy Environ. Mater.*, 2020, **3**, 469-491.
2 M. S. Dresselhaus, G. Dresselhaus and P. C. Eklund, *Science of fullerenes and carbon nanotubes: their properties and applications*, Elsevier, 1996.

3 J. Geng, W. Zhou, P. Skelton, W. Yue, I. A. Kinloch, A. H. Windle and B. F. Johnson, *J. Am. Chem. Soc.*, 2008, **130**, 2527-2534.
4 C. M. Lieber and Z. L. Wang, *MRS Bull.*, 2007, **32**, 99-108.
5 L. W. Tutt and T. F. Boggess, *Prog. Quantum Electron.*, 1993, **17**, 299-338.
6 N. Sariciftci, L. Smilowitz, A. J. Heeger and F. Wudl, *Science*, 1992, **258**, 1474-1476.
7 M. Sathish and K. Miyazawa, *CrystEngComm*, 2010, **12**, 4146-1451.
8 J. Kastner, J. Paloheimo and H. Kuzmany, *Fullerene field-effect transistors*, Springer, Berlin, Heidelberg, 1993.
9 K. Ogawa, T. Kato, A. Ikegami, H. Tsuji, N. Aoki, Y. Ochiai and J. P. Bird, *Appl. Phys. Lett.*, 2006, **88**, 112109.
10 S. H. Lee, K. Miyazawa and R. Maeda, *Carbon*, 2005, **43**, 887-889.
11 P. Krusic, E. Wasserman, P. Keizer and I. Morton, *Science*, 1991, **254**, 1183.
12 R. M. Lucente-Schultz, V. C. Moore, A. D. Leonard, B. K. Price, D. V. Kosynkin, M. Lu, R. Partha, J. L. Conyers and J. M. Tour, *J. Am. Chem. Soc.*, 2009, **131**, 3934-3941.
13 J.-J. Yin, F. Lao, P. P. Fu, W. G. Wamer, Y. Zhao, P. C. Wang, Y. Qiu, B. Sun, G. Xing and J. Dong, *Biomaterials*, 2009, **30**, 611-621.
14 J. Okuda-Shimazaki, S. Nudejima, S. Takaku, K. Kanehira, S. Sonezaki, and A. Taniguchi, *Health*, 2010, **2**, 1456-1459.
15 J. Song, X. Jia, K. Minami, J. P. Hill, J. Nakanishi, L. K. Shrestha and K. Ariga, *Appl. Nano Mater.*, 2020, **3**, 6497–6506.
16 F. Hsieh, L. K. Shrestha, K. Ariga and S. Hsu, *Chem. Commun.*, 2017, **53**, 11024-11027.
17 H. Liu, Y. Li, L. Jiang, H. Luo, S. Xiao, H. Fang, H. Li, D. Zhu, D. Yu, J. Xu and B. Xiang, *J. Am. Chem. Soc.*, 2002, **124**, 13370-13371.
18 L. Wang, B. Liu, S. Yu, M. Yao, D. Liu, Y. Hou, T. Cui, G. Zou, B. Sundqvist, H. You and D. Zhang, *Chem. Mater.*, 2006, **18**, 4190-4194.
19 S. S. Babu, H. Möhwald and T. Nakanishi, *Chem. Soc. Rev.,* 2010, **39,** 4021-4035.
20 I. A. Solov'yov, J. Geng, A. V. Solov'yov and B. F. G. Johnson. *Chem. Phys. Lett.,* 2009, **472**, 166-170.
21 L. K. Shrestha, Q. Ji, T. Mori, K. Miyazawa, Y. Yamauchi, J. P. Hill and K. Ariga, *Chem. Asian J*, 2013, **8**, 1662-1679.
22 J. Geng, I. A. Solov'yov, W. Zhou, A. V. Solov'yov and B. F. Johnson, *J. Phys. Chem. C*, 2009, **113**, 6390-6397.
23 L. Wang, B. Liu, D. Liu, M. Yao, Y. Hou, S. Yu, T. Cui, D. Li, G. Zou, A. Iwasiewicz and B. Sundqvist, *Adv. Mater.*, 2006, **18**, 1883-1888.
24 M. Yao, B. M. Andersson, P. Stenmark, B. Sundqvist, B. Liu and T. Wågberg, *Carbon*, 2009, **47**, 1181-1188.
25 R. Céolin, J. L. Tamarit, D. O. López, M. a. Barrio, V. Agafonov, H. Allouchi, F. Moussa and H. Szwarc, *Chem. Phys. Lett.*, 1999, **314**, 21-26.
26 Y. Zhou and W. Zhou, *CrystEngComm*, 2012, **14**, 1449-1454.
27 K. Miyazawa, Y. Kuwasaki, A. Obayashi and M. Kuwabara, *J. Mater. Res.*, 2002, **17**, 83-88.
28 K. Miyazawa, Y. Kuwasaki, K. Hamamoto, S. Nagata, A. Obayashi and M. Kuwabara, *Surf. Interface Anal.*, 2003, **35**, 117-120.
29 K. Miyazawa, K. Hamamoto, S. Nagata and T. Suga, *J. Mater. Res.,* 2003, **18**, 1096-1103.
30 A. Masuhara, Z. Tan, M. Ikeshima, T. Sato, H. Kasai, H. Oikawa and H. Nakanishi, *CrystEngComm,* 2012, **14**, 7787-7791.
31 J. Minato and K. Miyazawa, *Carbon*, 2005, **43**, 2837-2841.
32 M. Sathish, K. Miyazawa, J. P. Hill and K. Ariga, *J. Am. Chem. Soc.*, 2009, **131**, 6372-6373.
33 K. Miyazawa, C. Hirata and T. Wakahara. *J. Cryst. Growth*, 2014, **405**, 68-72.
34 K. Miyazawa and K. Hotta, *J. Cryst. Growth*, 2010, **312**, 2764-2770.
35 M. Tachibana, K. Kobayashi, T. Uchida, K. Kojima, M. Tanimura and K. Miyazawa, *Chem. Phys. Lett.*, 2003, **374**, 279-285.
36 B. Jiang, Q. Tang, W. Zhao, J. Sun, R. An, T. Niu, H. Fuchsab and Q. Ji, *CrystEngComm*, 2020, **22**, 6287-6294.
37 K. Miyazawa, *Sci. Technol. Adv. Mater.,* 2015, **16,** 013502.
38 B. Xin, Y. Pak, S. Mitra, D. Almalawi, N. Alwadai, Y. Zhang and I. S. Roqan, *ACS Appl. Mater. Interfaces,* 2019, **11,** 5223-5231.
39 I. A. Ajia, Y. Yamashita, K. Lorenz, M. M. Muhammed, L. Spasevski, D. Almalawi, J. Xu, K. Iizuka, Y. Morishima, D. H. Anjum, N. Wei, R. W. Martin, A. Kuramata and I. S. Roqan, *Appl. Phys. Lett.,* 2018, **113,** 082102.
40 H. Wan, A. Rath, S. H. Yu, M. S. Tan, S. J. Pennycook and D. H. Chua. *Carbon Lett.*, 2020, **30**, 1-8.
41 K. Miyazawa, J. Minato, M. Fujino and T. Suga, *Diam. Relat. Mater.*, 2006, **15**, 1143-1146.
42 L. Chen, X. Pang and J. Zhao, *New J. Chem.,* 2019, **43**, 11524-11528.
43 A. M. Rao, P. Zhou, K. A. Wang, G. T. Hager, J. M. Holden, Y. Wang, W. T. Lee, X. X. Bi, P. C. Eklund, D. S. Cornett and M. A. Duncan, *Science*, 1993, **259**, 955-957.
44 Y. P. Sun, P. Wang and N. B. Hamilton, *J. Am. Chem. Soc.*, 1993, **115,** 6378-6381.
45 O. Kozak, M. Sudolska, G. Pramanik, P. Cigler, M. Otyepka and R. Zboril, *Chem. Mater.,* 2016, **28,** 4085-4128.
46 S. Leach, M. Vervloet, A. Despres, E. Breheret, J. P. Hare, T. J. Dennis, H. W. Kroto, R. Taylor and D. R. M. Walton, *Chem. Phys.*, 1992, **160,** 451-466.
47 V. Capozzi, T. Trovato, H. Berger and G. F. Lorusso, *Carbon,* 1997, **35**, 763-766
48 T. Rudalevige, A. H. Francis and R. Zand, *J. Phys. Chem. A.,* 1998, **102,** 9797-802.
49 L. K. Shrestha, J. P. Hil, T. Tsuruoka, K. Miyazawa and K. Ariga, *Langmuir,* 2013, **29,** 7195-7202.
50 S. I. Cha, K. Miyazawa, Y. K. Kim, D. Y. Lee and J. D. Kim, *J. Nanosci. Nanotechnol.*, 2011, **11,** 3374-3380.
51 X. Zhang, X. Zhang, K. Zou, C. S. Lee and S. T. Lee, *J. Am. Chem. Soc.*, 2007, **129,** 3527-3532.
52 M. Du, M. Yao, S. Chen, B. Sundqvist, X. Yang, R. Liu, B. Liu, B. Zou, T. Cui and B. Liu, *J. Raman Spectrosc.,* 2017, **48,** 437-442.
53 H. J. Byrne, W. K. Maser, W. W. Rühle, A. Mittelbach, W. Hönle, H. G. von Schnering, S. Roth and B. D. Movaghar, *Synth. Met.*, 1993, **54**, 265-272.
54 S. Jie, L. Fei-ming, Q. Shi-xiong, L. Yu-fen, P. Wen-ji, Z. Jian-ying and Y. Zhen-xin, *Acta Phys. Sin. (Overseas Edn),* 1995, **4,** 175-182.
55 K. Miyazawa, J. Minato, H. Zhou, T. Taguchi, I. Honma and T. Suga, *J. Eur. Ceram. Soc.*, 2006, **26**, 429-434.
56 M. Watanabe, K. Hotta, K. Miyazawa and M. Tachibana, *Journal of Physics: Conference Series*, IOP Publishing, Nagoya, 2009.
57 X. Zhang, Y. Ma, S. Fu and A. Zhang, *Nanomaterials,* 2019, **9,** 1647.
58 D. S. Bethune, G. Meijer, W. C. Tang and H. J. Rosen, 1990. *Chem. Phys. Lett.*, **174**, 219-222.
59 K. Hotta and K. Miyazawa, *Journal of Physics: Conference Series*, IOP Publishing, Nagoya, 2009.
60 K. Hotta and K. Miyazawa, *Nano*, 2008, **3**, 355-359.
61 A. Aota, A. Hibara and T. Kitamori, *Anal. Chem.*, 2007, **79**, 3919.
62 C. L. Ringor and K. Miyazawa, *Diam. Relat. Mater.*, 2008, **17**, 529-534.